Metabolic resistance of the tiger mosquito to pyrethroid insecticides in La Réunion Island likely results from local adaptation

Tiphaine Bacot[1†], Jean-Marc Bonneville[1†], Vincent Lacroix[2], Pascal Oberbach[2], Thierry Gaude[1], Louis Nadalin[1] Frederic Laporte[1], Nausicaa Habchi-Hanriot[3], Guillaume Dupuy[3], Cyrille Czeher[3], Michael C Fontaine[4,5], Frederic Boyer[1] and Jean-Philippe David[1*]

1 Laboratoire d'Ecologie Alpine (LECA, UMR 5553), Université Grenoble-Alpes (UGA), Université Savoie Mont-Blanc (USMB), CNRS, Grenoble, France. **2** Laboratoire de Biométrie et Biologie Evolutive (LBBE, UMR 5558), CNRS, INRIA Erable, Université de Lyon, Université Lyon 1, Villeurbanne, France. **3** Agence Régional de Santé de La Réunion (ARS), Direction de la Veille et de la Sécurité Sanitaires & Santé et Milieux de vie, Service de Lutte Antivectorielle, Saint-Clotilde, France. **4** Maladies Infectieuses et Vecteurs : Ecologie, Génétique et Contrôle (MIVEGEC, UMR 5290), Université de Montpellier (UM), CNRS, IRD, Montpellier, France. **5** Groningen Institute for Evolutionary Life Sciences (GELIFES), University of Groningen, Groningen, Netherlands. **†** Equal contribution.

* jean-philippe.david@univ-grenoble-alpes.fr

Abstract

The resistance of mosquitoes to insecticides is a valuable model system for studying the genetic bases of xenobiotic adaptation in insects. The spread of the Asian tiger mosquito *Aedes albopictus* combined to the massive use of pyrethroid insecticides to limit arbovirus transmission resulted in the rise of resistance in various continents. Here, we investigated the genetic mechanisms underlying the recent adaptation of this mosquito to deltamethrin in La Réunion island. Bioassays confirmed the presence of resistance alleles in field populations. The resistance phenotype was further enhanced in the laboratory following a few generations of controlled selection. Combining whole genome Pool-seq and RNA-seq revealed no evidence of target-site resistance mutations but the over-expression and variant selection of detoxification enzymes associated with pyrethroid metabolism including cytochrome P450s, transferases and ABC-transporters. Among over-expressed detoxification genes, only one was linked to a gene duplication while polymorphism data suggest most of them being trans-regulated. Genome-wide selection signatures revealed a 9 Mb inverted superlocus responding to insecticide selection whose phenotypical importance remains uncertain. Altogether, this study indicates that the multigenic metabolic resistance phenotype observed in this insular territory mainly results from local adaptation. From an applied perspective, this study provides a set of markers to track pyrethroid resistance in the tiger mosquito in the South-West Indian Ocean. As this region is subjected to

recurrent arbovirus outbreaks, the additive resistance phenotype that may arise from the introduction of *Kdr* mutations from other territories also calls for improving resistance surveillance at the regional scale.

Author summary

While novel vector control strategies are being developed, chemical insecticides remain widely used to control mosquitoes transmitting human diseases such as the Asian tiger mosquito. However, the recurrent use of insecticides resulted in the emergence of resistance which can ultimately affect vector control efficacy. Here, we investigate the genetic bases underlying the resistance of the Asian tiger mosquito to the pyrethroid insecticide deltamethrin in La Réunion island. By combining two complementary genomic approaches, we showed that resistance is mainly caused by an increased insecticide detoxification while classical 'Knock down resistance' mutations affecting the target of the insecticide were not detected. We also showed that resistance is underlain by multiple genetic changes spread across the genome, supporting the local selection of resistance rather than the introduction of resistance alleles. Furthermore, we identified a large inverted supergene responding to insecticide selection. This study provides valuable insights into the genetic bases of insecticide resistance, enabling the implementation of molecular makers to improve the tracking of insecticide resistance in this major mosquito vector across the Indian Ocean.

Introduction

Natural populations experience a variety of human-driven selective pressures, leading to their adaptation through the expression of complex phenotypes (1). Understanding the genetic mechanisms allowing them to adapt to such rapid environmental changes provides key knowledge for populations management (2–4). The evolution of insecticide resistance is a good example of how natural selection can mediate the rapid adaptation of natural populations to anthropogenic pressures as it occurs in a large number of insects (5,6). Beyond understanding the adaptative mechanisms, identifying resistance alleles also contributes to improving management strategies (7–9). However, the frequent co-occurrence of multiple resistance mechanisms and the diversity of genetic events underlying resistant phenotypes often makes the characterization of resistance alleles challenging (5,10).

Among insect vectors, *Aedes* mosquitoes pose a significant threat to public health because they transmit major arboviral diseases (11,12). Among them, the invasive Asian tiger mosquito *Aedes albopictus* (Skuse, 1894) is of particular importance because its spread contributed to the worldwide

66 re-emergence of arboviruses such as dengue and chikungunya (13). Although significant research
67 efforts are dedicated to develop vaccines targeting these arboviruses (14–16), outbreak prevention
68 still massively relies on insecticide-based vector control (17). Pyrethroid insecticides such as
69 deltamethrin are the most-used insecticides against Aedes mosquitoes (18). However, the adaptation
70 of mosquitoes to such insecticides can ultimately reduce the efficacy of vector control preventive
71 actions (19–22).

72 Pyrethroids disrupt nerve function by altering the opening kinetics of the voltage-gated sodium
73 channel (VGSC gene: ,23,24). Pyrethroid resistance can be the consequence of point mutations
74 affecting the VGSC gene, known as Knock-down resistance (*Kdr*) mutations (target-site resistance); a
75 decreased insecticide penetration mediated by cuticle modification (cuticle resistance); and
76 biodegradation of the insecticide through complex detoxification pathways (metabolic resistance: ,10).
77 *Kdr* mutations typically affect a few conserved amino-acid positions in the VGSC protein and are fairly
78 well characterized in *Aedes* mosquitoes (25–28). Conversely, the genetic bases of insecticide
79 detoxification are far less understood. Indeed, the diversity and redundancy of genes underlying
80 xenobiotic detoxification pathways often lead to various multigenic adaptive trajectories depending on
81 the local context (5,10,17,23). In insects, pyrethroid metabolism typically includes an initial phase
82 involving hydroxylation by cytochrome P450s and sometimes ester-bond hydrolysis by
83 carboxylesterases, followed by the conjugation of hydrophilic groups by glutathione S-transferases
84 (GSTs) and UDP-glycosyltransferases (UDPGTs), and the excretion of the insecticide itself or its
85 metabolites by ABC-transporters(29–31). Molecular changes underlying metabolic resistance to
86 pyrethroids frequently include the over-expression of detoxification enzymes and transporters
87 mediated by cis- or trans-regulation or by gene duplication although the selection of
88 enzyme/transporter variants showing an enhanced activity toward the insecticide has also been
89 described (6,32–35).

90 The recent spread of *Ae. albopictus* to all continents and its ecological shift to more urbanized areas
91 (12) led to its increased exposure to pyrethroid insecticides and ultimately to the selection of
92 resistance. Pyrethroid resistance was first reported in South-East Asia more than a decade ago (36–39)
93 followed by other Asian regions (40–42). In these regions the resistance phenotype was often related
94 to the presence of various *Kdr* mutation haplotypes (40,43,44), although metabolic resistance was also
95 detected (45–47). Resistance was then detected in Europe following the introduction of *Kdr* mutations
96 from Asia (48–50). Resistance was also detected in Africa in association with *Kdr* mutations and
97 increased detoxification though the underlying resistance alleles were not characterized (51–53).

98 In the Indian Ocean, *Ae. albopictus* was likely imported from Asia in La Réunion island during the 17th
99 and the 18th centuries though other introductions likely occurred later (54). This mosquito was

100 associated to the chikungunya outbreak that occurred in 2005-2006 (55,56) and is the main vector of
101 recurrent dengue/chikungunya outbreaks since then (57). In La Réunion island, the recurrent use of
102 deltamethrin for vector control since 2006 ultimately resulted in the emergence of resistance as
103 detected by public health authorities in 2017 (58). However, the mechanisms underlying the
104 resistance phenotype have not been thoroughly investigated since then. A single heterozygote for the
105 V1016G *Kdr* mutation was observed from mosquitoes collected in La Réunion in 2016 as part of a
106 worldwide *Kdr* screening study (59). However, the circulation of *Kdr* mutation in the island or
107 neighbouring territories was not confirmed after this observation.

108 In this context, the present work aims at deciphering the genetic bases of the deltamethrin resistance
109 phenotype observed in *Ae. albopictus* populations in La Réunion island. This was achieved by adopting
110 an experimental design combining field populations and field-derived lines enriched or not for
111 resistance alleles by controlled selection. At the molecular level, an integrated genomic approach
112 combining RNA-seq and whole genome Pool-seq was applied to pinpoint resistance alleles and their
113 underlying genomic events. The evolutionary scenario leading to the emergence of resistance in La
114 Réunion island is then discussed in regards of the worldwide distribution of resistance alleles and the
115 local demographic context. While providing a set of novel molecular markers to track insecticide
116 resistance in this mosquito vector, the present study contributes to anticipate the emergence of
117 insecticide resistance in the South-West Indian Ocean region and its consequences for vector control
118 strategies.

119

120 Results

121 Deltamethrin resistance alleles circulate in La Réunion island

122 In order to improve the identification of deltamethrin resistance alleles, an experimental design
123 combining field populations and the controlled selection of a composite line was used (**Fig. 1A,** see
124 methods). Comparative deltamethrin bioassays performed on three field populations confirmed the
125 presence of resistance alleles in La Réunion (**Fig. 1B**). The three field populations (Saint-Paul, Saint-
126 Louis and Sainte-Suzanne) showed a significant decreased mortality to deltamethrin compared with
127 the susceptible SRun reference line. As expected, the composite line maintained without deltamethrin
128 selection for 6 generations (NS line) showed a resistance level similar to field populations. Selecting
129 the composite line for 5 generations with deltamethrin (Sel line) resulted in its increased resistance as
130 compared to the NS line, suggesting that resistance alleles are not fixed in the field and have been
131 further selected by controlled-selection in the laboratory.

132

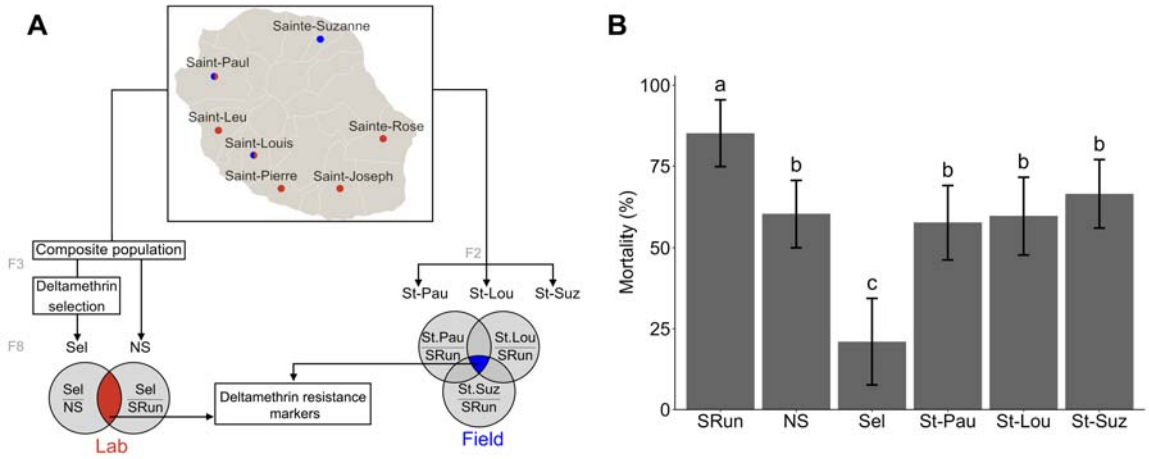

Fig 1. Study design and deltamethrin resistance levels. (A) Sampling sites and study design. The map shows the location of populations used to create the composite population from La Réunion island (red dots) and field populations (blue dots) used for analyses. For each line/population, the generation used is indicated. Venn diagrams illustrate the pairwise comparisons made for the identification of deltamethrin resistance markers (see methods). **(B)** Deltamethrin resistance levels. Mean mortality rates were obtained from standard WHO test tube assays using 0.03% deltamethrin impregnated papers. Error bars denote SD. Distinct letters indicate significantly distinct mortality rates (Conover-Iman test; N = 9; P value ≤ 0.05). Sel: deltamethrin selected line; NS: non-selected line; St-Pau: Saint-Paul; St-Lou: Saint-Louis; St-Suz: Sainte-Suzanne; SRun: susceptible reference line from La Réunion.

The resistance phenotype is not associated with target-site mutations

Whole genome pool-seq data from all lines were used to screen for *Kdr* mutations affecting the VGSC gene encoding the biochemical target of deltamethrin. Among the 132 polymorphisms detected in coding regions, six were non-synonymous (**S1 file**), but none matched the position of *Kdr* mutations previously associated with pyrethroid resistance in *Ae. albopictus* (i.e. V410L, L982Y, S989P, I1011M, V1016G/I, I1532T, and F1534C: ,28). In addition, these six non-synonymous variants are unlikely to contribute to deltamethrin resistance as they do not show a frequency pattern consistent with deltamethrin resistance across all lines. Furthermore, they were located in cytosolic regions being distant from the protein domains carrying known *kdr* mutations. Altogether, this indicate that the detected protein variants are most likely neutral, and that *Kdr* mutation do not contribute to deltamethrin resistance in La Reunion island.

Resistance involves the over-transcription of detoxification enzymes

RNA-seq performed on adult females enabled the detection of 13,918 genes passing coverage threshold which included 697 resistance candidate genes. Differential transcription analysis identified 48 genes differentially transcribed in association with resistance when considering both lab and field comparisons (**Fig. 2A and S2 Table**). The 12 under-transcribed genes include a single candidate encoding an ABC-transporter (LOC109429564). Conversely, the 36 over-transcribed genes included 11

159 candidates, representing a significant enrichment compared with the global gene set (from 5% to
160 30.5%, X^2 test $p < 0.05$). All of them belong to three gene families classically involved in pyrethroid
161 metabolism (P450s, transferases and ABC-transporters), leading to a significant enrichment of
162 detoxification genes (from 54% to 100%, X^2 test $p < 0.05$; **Fig. 2B**). All over-transcribed candidate genes
163 were located on chromosomes 1 and 2, some of them being clustered together (**Fig. 2C**). Several of
164 them show high protein homology with genes previously involved in pyrethroid resistance in *Aedes*
165 *aegypti* or *Anopheles gambiae*. The P450s *CYP6d5* (LOC115259486) was previously found over-
166 transcribed in resistant *Ae. albopictus* populations from China (same gene named CYP6A8 in 47) and
167 shows high homology with members of the CYP6Z subfamily previously involved in pyrethroid
168 metabolism (60–62). The P450 *CYP6a14* (LOC109421559) shows high homology with members of the
169 CYP6M subfamily validated as pyrethroid metabolizers in Anopheles mosquitoes (62,63). Similarly,
170 *GST-1* (LOC109412993) and *GST4*-like (LOC109413318) showed high homology with *theta*- and *delta*-
171 GSTs previously associated with pyrethroid in mosquitoes (45,64–67). Finally, the two ABC-
172 transporters (LOC109407008 and LOC109429691) showed a high homology with the ABCC subfamily
173 previously associated with pyrethroid resistance (68–73). Altogether, these results indicate that in
174 absence of *Kdr* mutations, the deltamethrin resistance phenotype observed in La Réunion island is
175 associated with an over-expression of detoxification enzymes likely involved in insecticide metabolism.

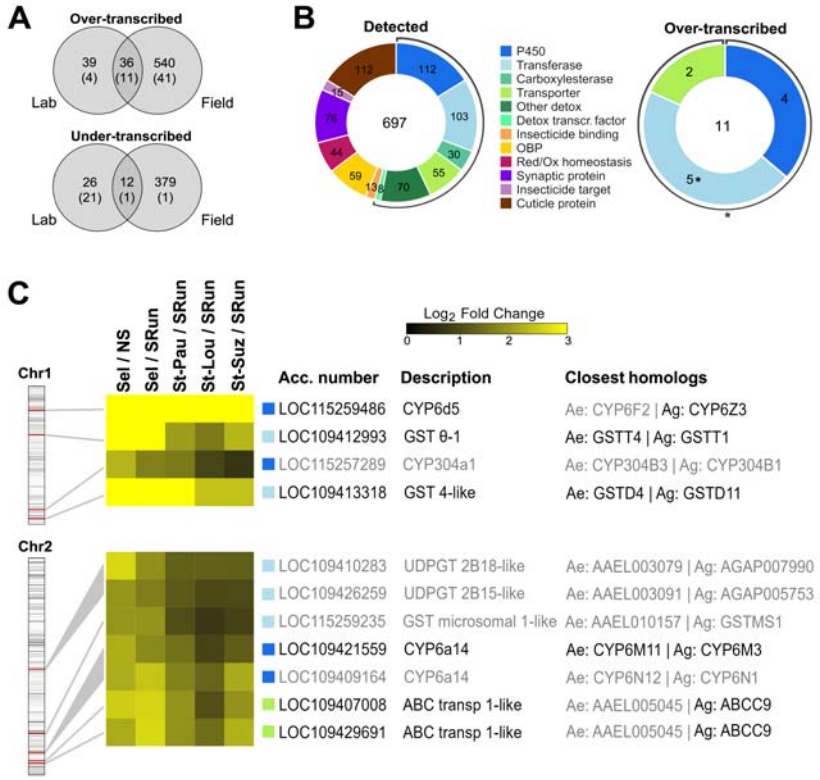

176

177 **Fig 2. Genes identified as differentially transcribed in association with deltamethrin resistance**. Only genes showing
178 consistent transcription level variations in both Lab and Field comparisons were considered associated with resistance (see
179 methods). **(A)** Venn diagrams showing the number of genes being differentially transcribed in association with resistance.
180 Numbers within brackets stand for candidate genes. **(B)** The left donut-chart describes all candidates genes detected by RNA-
181 seq and their respective gene families. The right donut-chart shows candidate genes associated with resistance. Black circular
182 arcs indicate gene families classically associated with detoxification. Stars indicate a significant enrichment from 'detected' to
183 'resistance associated' candidate genes (X^2 test, p value ≤ 0.05). **(C)** Candidate genes over-transcribed in association with
184 deltamethrin resistance. Log_2 fold changes obtained from each comparison are shown on the heatmap (scale from 0 to 3, see
185 S2 table for exact values). Colour squares refers to candidate gene families. Chromosomal positions are shown on the left
186 with the density of detected candidate genes shown as grey intensity. For each gene, NCBI accession number and description
187 are provided together with closest protein homologs in *Ae. aegypti* and *An. gambiae*. Genes in bold are those from which
188 close orthologs were previously associated with pyrethroid resistance. CYP: cytochrome P450; GST: glutathione S-transferase;
189 UDPGT: UDP-glycosyltransferase; ABC transp: ABC transporter; Sel: selected line; NS: non-selected line; St-Pau: Saint-Paul; St-
190 Lou: Saint-Louis; St-Suz: Sainte-Suzanne; SRun: susceptible reference line from La Réunion.

191 **Resistance is likely not associated with alternative splicing**

192 Using a *de novo* RNA-seq assembly strategy, we searched for alternative splicing events associated
193 with resistance. This analysis identified 166 events associated with resistance affecting 163 genes (**S3**
194 **Table**). This included 8 alternative splicing events, 4 large intron retention events (>50 bp) though
195 none of them affected candidate genes. Such analysis also identified 161 short genomic indel events (≤
196 50 bp) among with two affected candidate genes: the transcription factor HR96 LOC109416347 (6 bp
197 indel) and the peroxiredoxin LOC109415663 (3 bp indel). Altogether, these data indicate that
198 resistance in la Réunion does not strongly rely on alternative splicing events.

199 **An over-transcribed P450 is likely affected by a genomic duplication**

200 As over-transcription can be caused by an increased copy number, whole genome pool-seq data were
201 used to identify genes affected by copy number variations (CNV) in association with resistance based
202 on their increased exonic read coverages (see Methods). This analysis identified 72 genes showing an
203 increased coverage associated with resistance. Five of them were also over-transcribed in resistant
204 lines including the P450 *CYP6d5* (**Fig. 3A and 3B; S4 Table**). Comparing normalized coverage profiles at
205 the *CYP6d5 locus* revealed an increased coverage in resistant lines, which supports the occurrence of a
206 ~60 Kb duplication (**Fig. 3C**). The putative breakpoints were poorly covered, likely due to the presence
207 of transposable elements which were annotated as a LTR element on the left and a Line/R1 element
208 on the right.

209

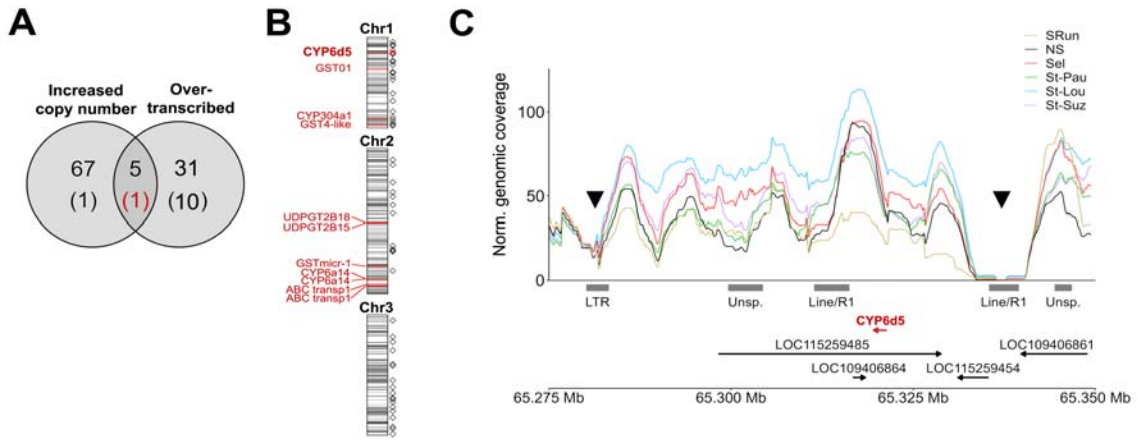

Fig 3. Gene copy number variant analysis. (A) Genes showing an increased copy number (CNV) in association with deltamethrin resistance in regards of those identified as overtranscribed. Numbers within brackets refer to candidate genes. **(B)** Distribution of gene copy number variants along chromosomes. Diamonds show the chromosomal position of the 72 genes showing an increased CNV associated with resistance. The red diamond refers to the candidate gene *CYP6d5* (LOC115259486). Over-transcribed candidate genes are named and shown as red marks in respect to candidate genes density (grey intensity). **(C)** Normalized read coverage profiles observed at the vicinity of *CYP6d5*. Normalized coverage profiles were computed for each line from whole genome pool-seq reads and smoothed using a 5 kb sliding window. The probable range of the duplicated region is delimited by black triangles. The *CYP6d5* gene is shown in red. Repeat masker annotation is shown as grey boxes. Genomic coordinates refer to AALBF3.v2 assembly. Sel: selected line; NS: non-selected line; St-Pau: Saint-Paul; St-Lou: Saint-Louis; St-Suz: Sainte-Suzanne; SRun: susceptible reference line from La Réunion.

Resistance is related to the selection of detoxification enzyme variants

Whole genome Pool-seq data were used to look for non-synonymous variants associated with resistance based on their frequency variation across resistant and susceptible lines. This analysis detected 197,403 non-synonymous variants passing coverage threshold with 11,679 of them affecting candidate genes (**Fig. 4A**). Among the 455 non-synonymous variants associated with resistance, 36 of them affected 27 distinct candidate genes **(Fig. 4B, S5 Table)**. A significant enrichment of candidate genes involved in detoxification was observed, mainly driven by a strong enrichment of P450s (from 15% to 33.3%, X^2 test $p < 0.02$). The 36 variants affecting candidate genes were spread over the three chromosomes (**Fig. 4C**). None of them affected over-transcribed genes though some were located in the same gene cluster. This was the case for the P450 *CYP6a8* variant located within a large CYP6 cluster which also include the two over-transcribed *CYP6a14* genes. Four major loci gathering multiple variants were identified in chromosome 3. The first one carried 4 variants affecting a *CYP4v2* and an ABC transporter. The second one included 9 variants affecting 6 P450s belonging to a cluster of 18 *CYP4C* genes. The last two gathered various candidate genes including a *CYP9f2* gene and an epoxide. Altogether, this analysis indicates that the deltamethrin resistance phenotype observed in La Réunion

is not only caused by the overtranscription of detoxification genes but also by the selection of protein variants likely related to insecticide metabolism.

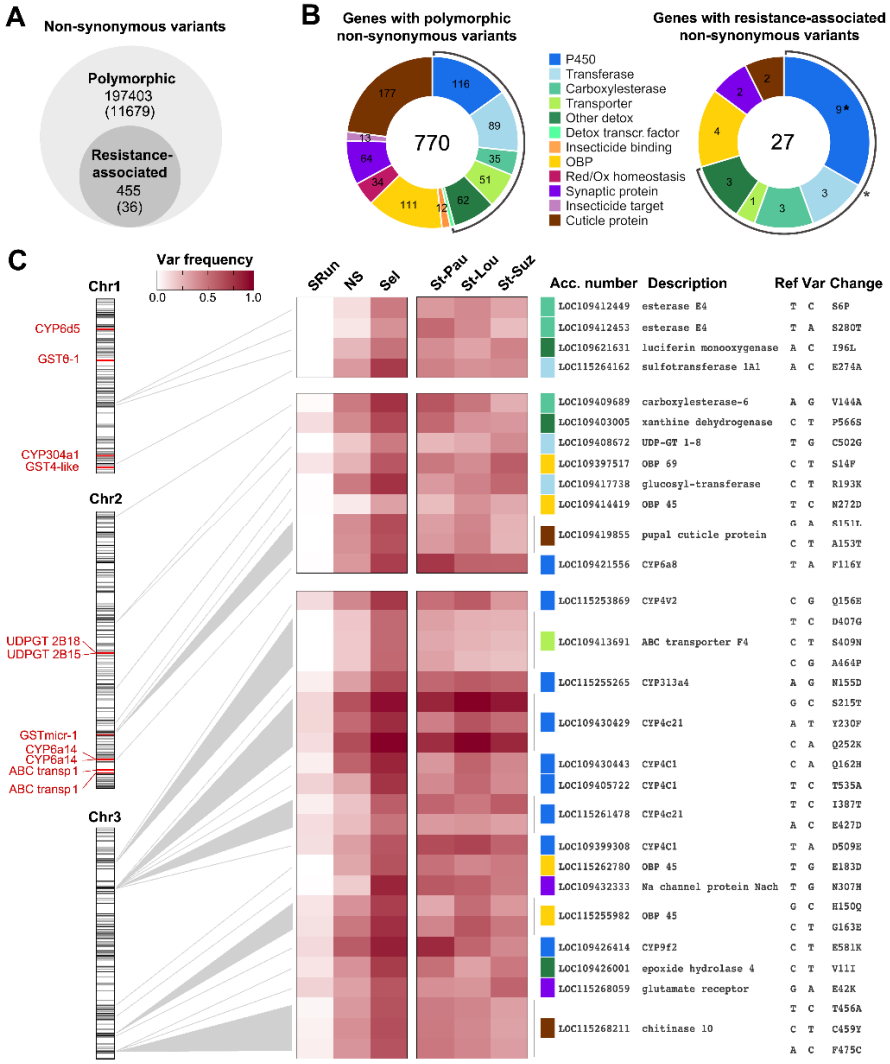

Fig 4. Protein variants associated with resistance. (A) Overview of non-synonymous variants identified. Numbers within brackets refer to variants affecting candidate genes. Variants associated with resistance were identified based on allele frequency variations across resistant and susceptible lines (see Methods) **(B)** The left donut-chart describes all candidate genes from which polymorphic non-synonymous variants were detected. The right donut-chart described those associated with resistance. Black circular arcs highlight gene families associated with detoxification. Stars indicate a significant enrichment (X^2 test, p value ≤ 0.05). **(C)** Candidate genes with non-synonymous variants associated with resistance. The heat map shows the frequency of the variant allele across all lines. The chromosomal position of each variant is shown on the left in respect to over-transcribed candidate genes (red marks) and candidate gene density (grey intensity). For each variant, gene family (colour square), gene accession number, gene description, nucleotide and amino-acid change are indicated. CYP: cytochrome P450; GST: glutathione S-transferase; UDPGT: UDP-glycosyltransferase; ABC transp: ABC transporter; Sel:

252 selected line; NS: non-selected line; St-Pau: Saint-Paul; St-Lou: Saint-Louis; St-Suz: Sainte-Suzanne; SRun: susceptible
253 reference line from La Réunion.

254

255 **Over-transcribed detoxification genes are not under direct selection**

256 Exonic polymorphism data were then used to look for gene-based selection signatures across the
257 genome between the Sel and NS lines based from allele frequency differentiation indexes (see
258 Methods). Among the 11 over-transcribed candidate genes, only the P450 *CYP304c1* and the
259 microsomal *GST-1* showed high differentiation indexes, which supports their cis-regulation. Other
260 over-transcribed candidate genes were below the baseline, consistent with their trans-regulation (**Fig.**
261 **5A**). Conversely, most candidate genes carrying protein variants associated with resistance showed
262 high gene differentiation indexes, supporting selection acting on the same *loci*. Among candidate
263 genes, those showing the highest differentiation indexes included two carboxylesterases *E4-like* on
264 chromosome 1, two UDPGTs and the *CYP6a8* P450 on chromosome 2, and the ABC transporter *F4* and
265 the two *CYP4c1* P450s on chromosome 3. Overall, though genetic drift may have occurred between
266 the Sel and NS lines, the high differentiation indexes observed across the three chromosomes support
267 the hypothesis of a multigenic adaptation based on standing genetic variation in La Réunion island (**Fig.**
268 **5B**).

269 **An inverted superlocus is under deltamethrin selection in La Réunion**

270 This analysis also identified a hundred genes located within an intriguing region of chromosome 2
271 displaying very high differentiation levels (**Fig. 5C and S6 Table**). This large 9.6 Mb *locus* showed a
272 strong selection signal in the Sel/NS comparison but also in other 'resistant *vs* susceptible'
273 comparisons coherent with a low recombination rate. Indeed, a quarter of the 3141 non-synonymous
274 polymorphisms detected in this region are above the whole genome top centile for Sel/NS
275 differentiation indexes. Examining reads topology identified 'one mate swap' read pairs and split reads
276 supporting the presence of a large genomic inversion whose breakpoints were 120,519,062 and
277 130,178,023. The partial mapping of these reads at the breakpoints together with the unmapped
278 fragments matching to multiple genomic locations supported the flanking of this inversion by two
279 transposable elements. The presence of this inversion at low frequency in the susceptible reference
280 strain SRun also suggests its pre-existence prior to its selection by deltamethrin in La Réunion. Among
281 the 107 genes located within the inverted region, only four belong to candidate genes including two
282 ABC-transporters, a cytochrome b5-like and a cuticle protein. However, none of them were
283 differentially transcribed, affected by CNV, or carried non-synonymous variants associated with
284 deltamethrin resistance. Among other genes located within the inversion, none showed a clear
285 association with a known resistance mechanism. Fifteen genes encoded known or putative (*i.e.* zing

finger proteins) transcription factors although none were previously associated with detoxification enzymes regulation. Several polymorphisms showing the highest Sel/NS differentiation affected the uncharacterized gene LOC115268503. Protein homology suggest that this gene encodes a S/T protein phosphatase with ankyrin motifs. As the voltage-gated sodium channel targeted by pyrethroids can be regulated by phosphorylation and interact with ankyrins (74,75), this gene is an attractive candidate to explain the selection of this large inversion by deltamethrin.

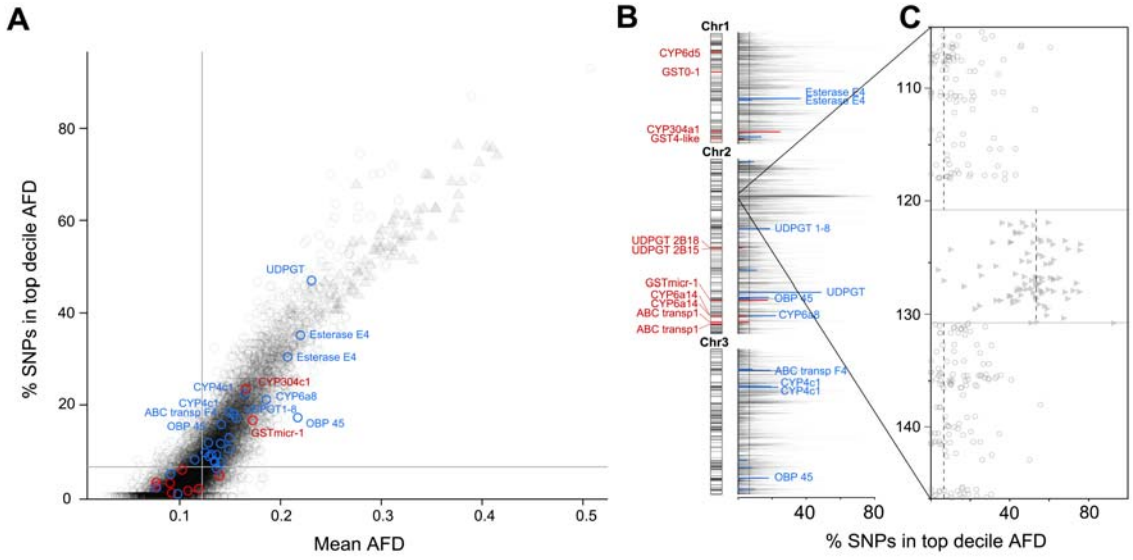

Fig 5. Genome-wide allele frequency differentiation. (A) The plot shows two genetic differentiation indexes for the Sel/NS line comparison: the mean Allele Frequency Difference per gene (mean AFD, absolute value) and the proportion (%) of SNPs per gene showing an AFD within the top decile of the global distribution (% SNPs in top decile AFD). These differentiation indexes were computed for the 10,192 protein-coding genes carrying >20 bi-allelic substitutions (see Methods). Median values are shown as grey lines. Candidate genes within top quartiles for both differentiation indexes are annotated with those differentially transcribed in association with resistance in red and those carrying protein variants associated with resistance in blue. Triangles denotes genes carried by the genomic inversion identified in chromosome 2. **(B)** Genome wide overview of the '% SNPs in top decile AFD' index for the Sel/NS comparison. The dashed line stands for the median of the differentiation index across all genes. The chromosomal position of candidate genes associated with resistance is shown together with candidate gene density (grey intensity). **(C)** Focus on the genomic region carrying the 9 Mb inversion associated with resistance. The '% SNPs in top decil AFD' index is shown for all genes. Horizontal grey lines delimit the inverted region with breakpoints at Chr2:120,519,062-130178023 in AALBF3.v2 assembly (Chr2:405,097,032-416,198,432 in AALBF5 assembly). Vertical dashed lines show the median of the '% SNPs in top decile AFD' index within and outside the inverted region. The genomic scale is in Mb respective to AALBF3v2.

Discussion

Metabolic resistance likely emerged from local adaptation in La Réunion island

310 Bioassays performed on field mosquito populations from La Réunion island revealed a significant
311 deltamethrin resistance phenotype, confirming the rise of resistance observed since 2017 (58).
312 Considering that resistance may have remained undetected for some times, the emergence of
313 resistance may have begun a few years after deltamethrin was adopted for vector control following
314 the 2005-2006 chikungunya outbreak. The resistance level of the non-selected composite line was
315 similar to those observed in the field, suggesting that the sampling design was efficient at capturing
316 resistance alleles circulating in the island. Indeed, the ancient colonization of this insular territory by
317 *Ae. albopictus* was linked to a high local genetic diversity with significant gene flows between
318 populations (76–78).

319 More than 30 non-synonymous polymorphisms affecting the VGSC targeted by deltamethrin have
320 been identified in *Ae. albopictus* worldwide but only a few were consistently associated with
321 pyrethroid resistance (23,26,28,V1016G, I1532T and F1534S/C/L: ,79). Despite the sequencing of large
322 mosquito pools at high coverage, none of these *Kdr* mutations was detected in La Réunion island,
323 either in field populations or in composite laboratory lines. Considering the recurrent usage of
324 deltamethrin since 2005, this supports the absence of *Kdr* mutations in La Réunion at the time of the
325 study. As *Kdr* mutations have already spread across multiple continents including Asia, Europe and
326 Africa (26,28), such result also confirm that limited gene flow occurred from these regions. Instead, a
327 multigenic metabolic resistance phenotype was observed, involving detoxification genes belonging to
328 families involved in pyrethroid metabolism such as cytochrome P450s, glutathione S-transferases,
329 UDP-glycosyl transferases, and ABC-transporters (31,80). Elevated detoxification enzyme activities
330 have been linked to deltamethrin resistance in *Ae. albopictus* populations from various regions (46,81–
331 84).

332 Transcriptomic screenings revealed the over-transcription of the same detoxification gene families in
333 *Ae. albopictus* resistant populations from Asia with some P450s being functionally validated (Ishak et
334 al. 2016, Xu et al. 2018, Zhou et al. 2024). Among the detoxification genes identified in La Réunion,
335 only the P450 (CYP6d5) was previously identified as contributing to deltamethrin resistance in *Ae.*
336 *albopictus* (same CYP gene named CYP6A8: ,47). Yet, several of them showed high protein homology
337 with known pyrethroid resistance genes identified in other mosquito species. This includes two P450s
338 showing high homology with *CYP6Ms/CYP6Zs* subfamilies, two GSTs likely belonging to GST-theta and -
339 delta families and two ABC-transporters likely belonging to the ABCC family. Although functional
340 validation is needed to clarify their importance in the overall phenotype, the emerging picture is the
341 independent selection of detoxification genes in Asia and La Réunion. Such hypothesis is also
342 supported by the absence of *Kdr* mutations previously detected in Asia in La Réunion island. Such
343 parallel evolution of detoxification genes under pyrethroid selection is probable considering the

344 functional redundancy observed within these gene families whose members are often organized in
345 clusters of genes sharing a high homology (10,85). Altogether, while the introgression of metabolic
346 resistance alleles cannot be ruled out, the genetic isolation of La Réunion island together with the
347 absence of *Kdr* mutations and the specific nature of the genes identified support their local selection
348 from standing genetic variation.

349 **Multiple genetic events underly the resistance phenotype**

350 Gene duplications mediating the over-expression of detoxification genes have been frequently
351 associated with the rapid adaptation of mosquitoes to insecticides (32,35,86,87). Here, the over-
352 transcribed P450 *CYP6d5* was linked to the presence of a ~100 Kb genomic duplication. Although our
353 short-read Pool-seq data did not allow to fully resolve the genomic architecture of the duplicated
354 locus, its flanking by transposable elements (TEs) was not surprising as TE-movements are often
355 associated with genomic duplication events (86,88), especially in TE-rich genomes such as *Aedes*
356 mosquitoes (89–91). No such duplication was identified for the other over-transcribed detoxification
357 genes, implying that their over-transcription is rather mediated by cis- or trans-regulation. In this
358 regard, the nuclear receptors CncC/Maf and AhR-ARNT considered as key regulators of insect
359 detoxification genes (92) were not differentially transcribed nor affected by protein variants in
360 association with resistance. Nevertheless, a two-codons deletion variant affecting the transcription
361 factor HR96 showed an increased frequency in resistant lines. The contribution of this transcription
362 factor to the regulation of detoxification enzymes has been demonstrated in spider mites (93,94).
363 Although this requires further validation, this finding supports the potential role of HR96 in the
364 regulation of detoxification enzymes in *Ae. albopictus*.

365 As metabolic resistance may also be the consequence of the selection of proteins variants showing a
366 higher activity toward the insecticide (10), polymorphism data were screened for non-synonymous
367 variants associated with resistance. Such analysis identified multiple detoxification protein variants
368 with P450s being over-represented. Yet this gene set showed no overlap with over-transcribed genes,
369 suggesting that these two adaptive mechanisms contribute to the multigenic resistance phenotype
370 observed in La Réunion island. Indeed, in a context of local adaptation, it is expected that selection
371 retains any polymorphism that contribute to resistance, affecting both gene expression and protein
372 function. Of particular interest was the selection of multiple P450 variants belonging to a cluster of 18
373 *CYP4C-like* genes on chromosome 3. Indeed, while *CYP4s* are not considered as classical xenobiotic
374 metabolizers in mosquitoes as opposed to *CYP6s*, *CYP9s*, some of them have been shown to be over-
375 transcribed in association with pyrethroid resistance in *Ae. aegypti* (95), suggesting their possible
376 contribution to deltamethrin metabolism. Similarly, the identification of two carboxylesterase variants
377 associated with resistance may indicate that these enzymes can still be active on deltamethrin or its

378 metabolites, even though the cyano group of type II pyrethroids like deltamethrin is thought to protect
379 the ester bond from a direct hydrolysis (96).

380 Polymorphism data were then used to look for genes under positive selection in association with
381 resistance. As expected, a good proportion of detoxification protein variants associated with resistance
382 showed a positive selection signal at the gene level. On the other hand, apart from one P450 and one
383 GST, most over-transcribed detoxification genes showed poor selection signals, supporting their trans-
384 regulation. Unexpectedly, such analysis also identified a large ~9 Mb genomic inversion on
385 chromosome 2 behaving as a supergene under deltamethrin selection. Genomic inversions can play a
386 key role in local adaptation as demonstrated in various biological models (97–100). Whether this
387 genomic event is specific to the South-West Indian Ocean or more widely distributed remains to be
388 investigated. In that concern, the identification of the inversion breakpoints will facilitate its high-
389 throughput genotyping by PCR. The hundred genes carried by the inverted locus included four
390 candidates but none of them were directly associated with deltamethrin resistance, suggesting that
391 they do not drive its selection. Considering the strong genetic linkage of the inverted haplotype,
392 deciphering which gene(s) drive the selection of this supergene is not at reach from the current data
393 set and requires functional approaches.

394 **A warning bell for the South-West Indian Ocean**

395 The French territory of La Réunion island is a hotspot of arbovirus transmission in the South West
396 Indian Ocean in line with a high human density and the presence of *Ae. albopictus* (57). Such
397 epidemiological context led to the recurrent use of deltamethrin for vector control since the first
398 Chikungunya outbreak of 2005-2006. In a context of genetic isolation, this repeated insecticide
399 pressure resulted in the local selection of a metabolic resistance phenotype underlain by various
400 genetic events. Such evolutionary scenario is supported by the multigenic nature of the phenotype
401 together with the striking absence of *Kdr* mutations, which are already widely distributed in this
402 species (26,28). At the time of the study, the resistance phenotype observed in the field was moderate
403 and can be further increased following a few generations of deltamethrin exposure, suggesting that
404 the selection of resistance alleles is undergoing in La Réunion and might be counterbalanced with
405 fitness costs. As the selection of this multigenic resistance phenotype may affect various mosquito life
406 traits including vector competence (7,101), precising its impact on population dynamics and viral
407 transmission is of interest.

408 Considering that the selection process was undergoing by the time of the study, the intense vector
409 control activity associated with recent chikungunya and dengue outbreaks may have resulted in an
410 increased frequency of resistance alleles in La Réunion and their dispersal to other neighbouring
411 territories of the South-West Indian Ocean. In addition, although *Kdr* mutations were not detected by

412 the time of the study, their introduction from Europe, Asia or Africa should be considered as a major
413 risk for the region. Indeed, their introduction in populations already carrying metabolic alleles is
414 expected to lead to an additive resistance phenotype that may impact vector control efficacy, as
415 shown in *Ae. aegypti* (19,21). In this context, the present study calls for an improved surveillance of
416 pyrethroid resistance in this region. Ideally, this surveillance should combine annual bioassays on
417 sentinel populations and the tracking of key metabolic resistance alleles identified here together with
418 known *Kdr* mutations.
419

420 ## Methods

421 **Mosquito lines and experimental design**

422 All mosquito lines were maintained under standard insectary conditions (27 ± 2°C, 70 ± 10 % relative
423 humidity and light/dark cycle 14h:10h). Populations size were maintained over 1000 individuals to
424 reduce the effect of genetic drift. Larvae were reared in tap water and fed with hay pellets. Adults
425 were maintained in mesh cages and fed on filter papers impregnated with a 10 % honey solution.
426 Blood feeding was conducted on mice to generate eggs of the next generation. Three days-old non-
427 blood-fed adult females were used for bioassays and molecular work.

428 The experimental design combined different mosquito populations all originating from La Réunion
429 island (**Fig. 1A**). First, a composite population from la Réunion island was created by pooling >500
430 larvae from six field populations collected in 2018-2019 using a minimum of three ovitraps per
431 population. After two generations of genetic mixing (F1 to F3), the composite population was split in
432 two separated lines (N>1000 in each line): the first being maintained without insecticide selection (NS
433 line) and the other being selected with deltamethrin for five successive generations (Sel line). Selection
434 was conducted on males and females separately prior mating as follows. Batches of 25 non-blood-fed
435 3-5 days-old adults were exposed to filter papers impregnated with 0.03% deltamethrin using WHO
436 test tubes. Exposure times were adjusted from 30 min to 1h to reach 40-60% mortality for each sex.
437 Surviving males and females were then pooled in a single mesh cage and allowed to reproduce.
438 Females were blood fed and allowed to lay eggs to generate the next generation. Three field
439 populations sampled in 2021 from the localities of St-Paul, St-Louis and St-Suzanne were also used.
440 Finally, the laboratory susceptible strain SRun colonized from La Réunion island in the 2000s was used
441 as reference line. For molecular analyses, genes and polymorphisms associated with resistance were
442 identified based on the five pairwise comparisons: 'Sel *vs* NS'; 'Sel *vs* SRun' and 'each field population
443 *vs* SRun'. Only genes and polymorphisms showing consistent variations (in the same direction) for all
444 comparisons were retained.

445 **Bioassays**

446 Comparative deltamethrin bioassays were performed on 3-5 days-old adult females following WHO
447 mosquito testing guidelines (102) using test tubes equipped with home-made insecticide papers
448 impregnated with 0.03% deltamethrin. Each bioassay was conducted using 9 replicates of 25 females
449 and an exposure time of 1h. Such insecticide dose resulted in a mortality >80% in the susceptible
450 reference line SRun. After insecticide exposure, mosquitoes were allowed to recover for 24h with a
451 cotton bowl impregnated with a 10% honey solution before mortality recording.

452 **Reference genome and candidate genes**

453 Genomic analyses were performed using the version AALBF3 of *Ae. albopictus* reference genome,
454 which was the latest available assembly at the time of this study (103). As this assembly was made
455 from 574 ordered scaffolds, the successive scaffolds were assembled into pseudo-chromosomes with
456 50N spacers (hereafter referred to as AALBF3.v2 assembly). A gff3 annotation file based on AALBF3.v2
457 assembly was also created based on AALBF3 annotation. The genomic coordinates of each scaffold on
458 AALBF3.v2 assembly is provided in **S7 Table**. Among the 22,435 features annotated in AALBF3.v2, only
459 the 17,342 genes and pseudogenes carried by the three nuclear chromosomes were retained for
460 genomic analyses. A subset of 953 genes belonging to 12 different families possibly involved in
461 insecticide resistance was defined. These candidate genes included: insecticide targets; synaptic
462 proteins; detoxification enzymes *sensu lato*; known detoxification transcription factors; ABC-
463 transporters; insecticide binding proteins; cuticle proteins; red/ox enzymes; odorant binding proteins
464 (**S8 Table**).

465 **RNA-sequencing**

466 For each line, four RNA-seq libraries were prepared from distinct batches of 25 five days-old non-
467 blood-fed females. Total RNA was extracted using TRIzol® (ThermoFisher Scientific) according to
468 manufacturer's instructions. RNA extracts were quantified with a Nanodrop One (ThermoFisher
469 Scientific) and diluted to meet sequencing requirements. Sequencing was performed by the BGI
470 Hongkong Tech Solution NGS Lab. Sample quality control was conducted on an Agilent 2100 and
471 libraries were prepared from 10 ng total RNA following the DNB-seq Eukaryotic Strand-specific mRNA
472 library protocol. Briefly, mRNAs were enriched with poly-A tails using oligodT beads and fragmented to
473 an average size of 200-400 bp before being reverse transcribed using random primers. Double-
474 stranded cDNAs were end-repaired and 3' adenylated. Adaptors were ligated at the 3'-end of the
475 cDNAs. Libraries were PCR amplified using rolling circle amplification to make DNA nanoballs (DNB)
476 and sequenced in multiplex as 100 bp paired-end reads. Adapters were trimmed with the SOAPnuke
477 v2.2.1 (104) and reads were filtered on base quality to reach an average Phred+33 score of 37. Quality

478 control was conducted using FastQC (105) leading to an average of 60.2 M quality-filtered reads per
479 replicate. Reads were then mapped onto the AALBF3.v2 assembly using STAR v2.7.10a (106) with
480 default parameters, except a minimum intron size of 10 bp. Mapping quality was assessed with
481 samtools v1.6 (http://www.htslib.org/), with an average of 94 % of reads being properly mapped (**S9**
482 **Table**). Gene read counts were quantified by STAR with default parameters.

483 *Differential transcription*

484 Differential transcription analysis was performed using DESeq2 (Love et al., 2014) on all genes and
485 pseudogenes showing ≥5 read counts in each of the four replicates for at least one mosquito line.
486 Differentially transcribed genes were identified based on their congruent transcription fold change (FC)
487 and adjusted Student' t-test *p* values (False Discovery Rate for multiple testing correction, 107) across
488 the five 'resistant vs susceptible' comparisons (see experimental design on **Fig. 1**). Fold change
489 thresholds were set as follows: FC ≥ 3 in 'Sel vs NS'; FC ≥ 3 in 'Sel vs SRun' and FC ≥ 1.5 in the three
490 'field vs SRun' comparisons while adjusted *p* Value threshold was set to 0.001 for all comparisons. In
491 order to clarify the role of detoxification genes over-transcribed in association with resistance, their
492 closest homologs were identified in *Ae. aegypti* and *An. gambiae* using a protein blast against *Ae.*
493 *aegypti* (LVP_AGWG) and *An. gambiae* (PEST) proteomes from VeuPathDB (108,109). As P450 gene
494 descriptions and gene names can vary across different genome versions, blast results were backed up
495 with a phylogenetic analysis performed on *CYP6s* protein sequences from *Ae. albopictus, Ae. aegypti*
496 and *An. gambiae*. Protein sequences were retrieved from NCBI and those having a validated role in
497 pyrethroid resistance were identified based on the literature and sequence alignments. Phylogenetic
498 trees were built using the only 'NGPhylogeny.fr' pipeline using approximate likelihood-ratio test (aLRT)
499 as branch support, with a *CYP4* sequence as outgroup (110).

500 *Alternative splicing*

501 Alternative splicing events and indels were identified from RNA-seq data using KisSplice v2.6.2 (111).
502 This *de novo* splicing events predictor was run on each replicate of each line with default parameters,
503 except the parameter -b which was set to 15 to account for the higher level of polymorphism in *Ae.*
504 *albopictus* compared with mammals. Splicing variants were identified with KissDE R package v1.19.0
505 (112). Only variants covered by at least 20 reads, affecting known genes and showing a congruent
506 splicing variation across all 'resistant vs susceptible' comparisons were retained. Delta Percent Spliced
507 In (ΔPSI) threshold were as follows: 20% for 'Sel *vs* NS'; 20% for 'Sel *vs* SRun' and 15% for the three
508 'field *vs* SRun' comparisons. The adjusted *p* value threshold was set to 0.05 (Benjamini & Hochberg
509 FDR for multiple testing correction). The splicing events passing these filters were then mapped to
510 AALBF3.v2 assembly using KisSplice2RefGenome v1.2.3

511 (https://kissplice.prabi.fr/tools/kiss2refgenome/) and assigned into three types: alternative splicing,
512 indels and intron retentions. The distinction between genomic indels and intron retention was based
513 on an arbitrary threshold (indel if ≤ 50 bp and intron retention if > 50 bp).

514 **Whole genome pool sequencing**

515 For each line, three batches of 33-35 three days-old virgin non-blood-fed females were sampled for
516 whole genome pool-sequencing (100 individuals per line). Genomic DNA was extracted separately for
517 each batch using the GENTRA Puregene kit (QIAGEN) following manufacturer's instructions quantified
518 using Qubit (Qiagen) and then pooled in equal DNA quantity. After quality check, one sequencing
519 library was prepared for each line following the DNBseq plant and animal whole genome resequencing
520 protocol (https://en.mgi-tech.com/products/). Briefly, DNA was fragmented, size selected (insert size
521 ~350 bp) and end-repaired. Adapters were ligated to the DNA fragments which were then size-
522 selected, amplified by PCR using rolling circle amplification and sequenced in multiplex as 150 bp
523 paired-end reads with the DNBseq Technology (MGI Tech Co). Sequencing reads were filtered based
524 on base quality resulting in a final average Phred score of 37 and adapters were removed with the
525 SOAPnuke software v2.2.1 (104) leading to an average of ~1630 M reads per line (**S9 Table**). Reads
526 were then mapped onto the *Ae. albopictus* AALBF3.v2 genome with BWA mem v0.7.17-r1188 (113).
527 SAM files were converted into BAM format, sorted by coordinates and unmapped reads were removed
528 using samtools v 1.6 (114). Mapped reads were trimmed and only reads showing a probability of
529 correct mapping of 0.999 were kept (MapQ ≥30). PCR duplicates were removed using picard
530 MarkDuplicates v2.27.5 (http://broadinstitute.github.io/*picard*), resulting in an average of 631 M
531 mapped reads per sample and a mean genome coverage of 64.2X.

532 *Copy number variations*

533 Genomic duplications were searched for by looking for genes showing a higher mean read coverage in
534 resistant than in susceptible mosquito lines. Though likely to generate false positives, this approach
535 was preferred to pipelines integrating local coverage variations and the presence of flanking non-
536 colinear reads (115) because the *Ae. albopictus* is genome is highly enriched with transposable
537 elements (>41% of the genome: ,89) likely to generate false negatives. Indeed, transposable elements
538 are frequent at duplication breakpoints leading to the loss of non-colinear reads (*e.g.* split reads and
539 both mate flip reads) due to multiple mapping events. Since intronic regions are highly variable and
540 thus more subject to local coverage variations, mean normalized gene coverages were computed from
541 exonic regions only. Fold changes of normalized exonic coverage between lines were computed for all
542 genes. Since very low gene coverage can lead to artefactual high coverage variations, genes showing a
543 normalized coverage lower than the 5% global quantile were not considered. Furthermore, a global
544 observation of the data set indicated that the dispersion of coverage variations increased for smaller

545 transcripts. To take this into account, a sliding windows approach considering transcript length was
546 applied to identify differentially covered genes: for each pairwise line comparison, a gene was
547 considered as affected by a positive copy number variation (CNV) when its normalized coverage
548 variation was higher than the 95% quantile of the variation observed from the 1000 genes showing the
549 most similar transcript lengths. Following this approach, genes were considered as showing a positive
550 CNV associated with resistance when passing this threshold for all 'resistant vs susceptible'
551 comparisons ('Sel *vs* NS', 'Sel *vs* SRun' and the three 'field *vs* SRun' comparisons).

552 *Gene polymorphisms*

553 Gene polymorphisms associated with resistance were searched for using reads mapped to the coding
554 regions of protein-coding genes. For each line, polymorphisms were called using bcftools-v1.17 (116).
555 We then retained biallelic variants showing a read coverage between 50 and 300 reads in all lines, a
556 frequency ≥15% in at least one line and a frequency variation ≥15% between at least two lines. Genic
557 effects were annotated according to the longest reading frame using snpEff v5.2c (117). As the
558 reference genome *Foshan* strain is susceptible to deltamethrin (118) variants were considered
559 associated with resistance if the frequency of the variant allele increased in 'resistant vs susceptible'
560 comparisons. Frequency thresholds were as follows: frequency ≤15% in the susceptible SRun line,
561 frequency variation ≥25% in 'Sel *vs* SRun' and in 'Sel *vs* NS' comparisons, and frequency variation ≥20%
562 in the three 'Field *vs* SRun' comparisons.

563 We also specifically searched for non-synonymous polymorphisms affecting the gene encoding the
564 voltage-gated sodium channel protein targeted by deltamethrin (VGSC-para gene carrying the Kdr
565 mutations). However, this gene was incorrectly assembled in AALBF3 likely due to uncontrolled
566 heterozygosity. Indeed, the previous AALFBF2 assembly (Palatini et al., 2020) contains two annotated
567 gene copies, each located in a different scaffold (the 'VGSC-para' LOC109421922, and the 'VGSC para-
568 like' LOC109432678*)*. In AALBF3, both genic sequences were present but the 'para' sequence was not
569 annotated as a gene. In the latest AALBF5 assembly, a better control of heterozygosity led to the two
570 contigs being merged, resulting in a single annotated 'VGSC-para' gene (LOC109421922). We therefore
571 assumed that the AALBF5 assembly is correct. In order to study the polymorphism of this gene, all
572 reads mapped to AALBF3.v2 in the *para* (Chr3:378648962-378932310) and *para-like* regions
573 (Chr3:377089613-377411247) were re-mapped to the AALBF5 gene LOC109421922 and SNPs were
574 called as described above.

575 *Selection signatures*

576 Polymorphisms data were also used to look for selection signatures associated with deltamethrin
577 resistance between the Sel and NS lines, which only diverged by 5 generations of deltamethrin

578 selection. This analysis was based on all exonic bi-allelic substitutions covered by 50 to 300 reads in
579 each line and being polymorphic between these two lines (*i.e.* showing a variant frequency from 5% to
580 95% in at least one line). From this dataset, two genetic differentiation indexes were computed at the
581 gene level: the mean Absolute Frequency Difference (mean AFD), and the percentage of SNPs in the
582 top decile of the overall genomic AFD distribution. These indexes were plotted against each other and
583 across the AALBF3.v2 genome for the 10192 protein-coding genes containing ≥20 substitutions.

584

585 ## Acknowledgments

586 This study was funded by the French Agency for Food, Environmental and Occupational Health &
587 Safety under the grant number EST-19-055. TB was supported by a PhD fellowship funded by the
588 Grenoble-Alpes University (UGA). The funders had no role in study design, data collection and
589 interpretation, or decision to submit the work for publication. We thank Dr. Julien Cattel for providing
590 the susceptible reference strain SRun. We also thank Vincent Lefort for help with phylogenetic
591 analyses.

592

593 ## Data availability

594 RNA-seq and WG Pool-seq sequencing data have been deposited at EBI short read archive (SRA) under
595 accession numbers E-MTAB-15418 and E-MTAB-15456.

596

597 ## Ethical aspects

598 Mice were kept in the animal facility of the Biology department of the University of Grenoble-Alpes,
599 approved by the French Ministry of Animal Welfare (agreement no. B 38 421 10 001) and used in
600 accordance with the laws of the European Union (directive 2010/63/EU). The use of animals for this
601 study was approved by the ComEth Grenoble-C2EA-12 ethics committee mandated by the French
602 Ministry of Higher Education and Research (MENESR). The study was conducted in accordance with
603 the ARRIVE guidelines.

604

605 ## Author contributions

606 **Conceptualization:** Tiphaine Bacot, Jean-Marc Bonneville, Jean-Philippe David
607 **Data curation:** Tiphaine Bacot, Pascal Oberbach, Vincent Lacroix, Jean-Marc Bonneville

608 **Formal analysis:** Tiphaine Bacot, Pascal Oberbach, Jean-Marc Bonneville, Jean-Philippe David
609 **Funding acquisition:** Jean-Philippe David
610 **Investigation:** Tiphaine Bacot, Pascal Oberbach, Thierry Gaude, Louis Nadalin, Frederci Laporte,
611 Guillaume Dupuy, Frederic Boyer
612 **Methodology :** Frederic Boyer, Vincent Lacroix, Tiphaine Bacot, Jean-Marc Bonneville, Jean-Philippe
613 David
614 **Project administration:** Jean-Philippe David
615 **Resources:** Nausicaa Habchi-Hanriot, Guillaume Dupuy, Cyrille Czeher
616 **Supervision:** Jean-Marc Bonneville and Jean-Philippe David
617 **Writing – original draft:** Tiphaine Bacot, Vincent Lacroix, Jean-Marc Bonneville, Jean-Philippe David
618 **Writing – review & editing:** Tiphaine Bacot, Michael C Fontaine, Jean-Marc Bonneville, Jean-Philippe
619 David
620

621 ## Supporting information

622

623 **S1 File. Polymorphisms in the VGSC gene.** The first xlsx sheet describes all polymorphisms detected in
624 the VGSC coding regions. For each polymorphism, the following information is provided: Position
625 relative to AALBF5 assembly; amino-acid position in respect to the longest isoform; genic effect;
626 variant allele frequency in each line; Variant allele frequency variations between resistant and
627 susceptible lines; number of reads supporting each allele for each line. The second xlsx sheet provides
628 a graphical overview of the position of the variant identified relative to transmembrane domains and
629 known Kdr mutations.

630 **S2 Table**. **Gene transcription data.** This table describes transcription data for all genes detected by
631 RNA-seq. For each gene the following information is provided: AALBF3 accession number;
632 chromosomal position relative to AALBF3.v2 assembly; coding strand; gene type; Candidate gene
633 family; baseMean (mean normalized read counts across all conditions); $\log_2$ fold change and adjusted P
634 value for each resistant/susceptible comparison.

635 **S3 Table. Alternative splicing.** For each splicing event identified, the following information is provided:
636 AALBF3 accession number; gene description; candidate gene family; chromosome; event start; event
637 end; event type and subtype; event size in bp; frameshift occurrence; mean coverage; percent spliced
638 in (PSI for each line); PSI variation (ΔPSI for each comparison).

639 **S4 Table. Gene copy number variations.** For each gene detected, the following information is
640 provided: AALBF3 accession number; chromosomal position relative to the AALBF3.v2 assembly;

641 coding strand; gene type; candidate gene family; gene description; mRNA length; normalized exonic
642 coverage (for each lines); mean normalized coverage across all lines; coverage filter; CNV status for
643 both lab and field comparisons.

644 **S5 Table. Non-synonymous variants associated with resistance.** For each variant, the following
645 information is provided: chromosomal position relative to AALBF3.v2 assembly; reference and variant
646 alleles; polymorphism type; AALBF3 gene accession number; gene description; candidate gene family;
647 longest transcript; variant exon rank; variant genic effect; amino-acid change; cDNA position relative to
648 cDNA length; amino-acid position relative to protein length; total coverage (for each line); variant
649 allele frequency (for each line).

650 **S6 Table. Gene differentiation indexes.** For each gene the following information is provided: Gene
651 accession number; chromosomal position relative to AALBF3.v2 assembly; coding strand; gene
652 description; candidate gene family; total number of polymorphic SNPs; number of synonymous SNPs;
653 number of non-synonymous SNPs; number of resistance-associated non-synonymous SNPs; mean
654 Allele Frequency Variation between Sel and NS Lines (mean AFD); the percent of SNPs showing an AFD
655 within the top decile of the global distribution (% top decil AFD); differential transcription associated
656 with resistance (Yes/No); gene being within the inversion identified on chr2 (Yes/No).

657 **S7 Table. The AALBF3.v2 genome assembly.** The genomic position of AALBF3 scaffolds on AALBF3.v2
658 chromosomes is provided. AALBF3 scaffolds were assembled in the same order as described in Boyle
659 et al. 2021 with 50N spacers inserted between them.

660 **S8 Table. Resistance candidate genes.** For each gene the following information is provided:
661 AALBF3accesion number; chromosomal position relative to AALBF3.v2 assembly; coding strand; gene
662 type; candidate gene family; gene description.

663 **S9 File. Sequencing data overview.** The first xlsx sheet provides RNA-seq sequencing and mapping
664 statistics. The second xlsx sheet provides whole genome Pool-seq sequencing and mapping statistics.

665

666 ## References

667 1. Orr HA. The genetic theory of adaptation: a brief history. Nat Rev Genet. 2005;6(2):119–27.

668 2. Hendry AP, Farrugia TJ, Kinnison MT. Human influences on rates of phenotypic change in wild
669 animal populations. Mol Ecol. 2008;17(1):20–9.

670 3. Hendry AP, Gotanda KM, Svensson EI. Human influences on evolution, and the ecological and
671 societal consequences. Philos Trans R Soc Lond B Biol Sci. 2017;372(1712).

672 4. Palumbi SR. Humans as the World's Greatest Evolutionary Force. Science.
673 2001;293(5536):1786–90.

674 5. Ffrench-Constant RH, Daborn PJ, Le Goff G. The genetics and genomics of insecticide resistance.
675 Trends Genet. 2004;20(3):163–70.

676 6. Liu. Insecticide Resistance in Mosquitoes: Impact, Mechanisms, and Research Directions. Annu
677 Rev Entomol. 2015;60(1):537–59.

678 7. Bass C, Jones CM. Editorial overview: Pests and resistance: Resistance to pesticides in arthropod
679 crop pests and disease vectors: mechanisms, models and tools. Curr Opin Insect Sci.
680 2018;27:iv–vii.

681 8. Dusfour I, Vontas J, David JP, Weetman D, Fonseca DM, Corbel V, et al. Management of
682 insecticide resistance in the major Aedes vectors of arboviruses: Advances and challenges. PLoS
683 Negl Trop Dis. 2019;13(10):e0007615.

684 9. Hawkins NJ, Bass C, Dixon A, Neve P. The evolutionary origins of pesticide resistance. Biol Rev
685 Camb Philos Soc. 2018;94(1):135-155.

686 10. Li XC, Schuler MA, Berenbaum MR. Molecular mechanisms of metabolic resistance to synthetic
687 and natural xenobiotics. Annu Rev Entomol. 2007;52:231–53.

688 11. Brown JE, Evans BR, Zheng W, Obas V, Barrera-Martinez L, Egizi A, et al. Human impacts have
689 shaped historical and recent evolution in *Aedes aegypti*, the dengue and yellow fever mosquito.
690 Evolution. 2014;68(2):514–25.

691 12. Paupy C, Delatte H, Bagny L, Corbel V, Fontenille D. Aedes albopictus, an arbovirus vector: from
692 the darkness to the light. Microbes Infect Inst Pasteur. 2009;11(14–15):1177–85.

693 13. Bonizzoni M, Gasperi G, Chen X, James AA. The invasive mosquito species Aedes albopictus:
694 current knowledge and future perspectives. Trends Parasitol. 2013;29(9):460–8.

695 14. Carvalho VL, Long MT. Perspectives on New Vaccines against Arboviruses Using Insect-Specific
696 Viruses as Platforms. Vaccines. 2021;9(3):263.

697 15. Garg H, Mehmetoglu-Gurbuz T, Joshi A. Virus Like Particles (VLP) as multivalent vaccine
698 candidate against Chikungunya, Japanese Encephalitis, Yellow Fever and Zika Virus. Sci Rep.
699 2020;10(1):4017.

700 16. Silva JVJ, Lopes TRR, Oliveira-Filho EFD, Oliveira RAS, Durães-Carvalho R, Gil LHVG. Current status,
701 challenges and perspectives in the development of vaccines against yellow fever, dengue, Zika
702 and chikungunya viruses. Acta Trop. 2018;182:257–63.

703 17. Moyes CL, Vontas J, Martins AJ, Ng LC, Koou SY, Dusfour I, et al. Contemporary status of
704 insecticide resistance in the major Aedes vectors of arboviruses infecting humans. PLoS Negl Trop
705 Dis. 2017;11(7):e0005625.

706 18. Van Den Berg H, Da Silva Bezerra HS, Al-Eryani S, Chanda E, Nagpal BN, Knox TB, et al. Recent
707 trends in global insecticide use for disease vector control and potential implications for
708 resistance management. Sci Rep. 2021;11(1):23867.

709 19. Dusfour I, Thalmensy V, Gaborit P, Issaly J, Carinci R, Girod R. Multiple insecticide resistance in
710 *Aedes aegypti* (Diptera: Culicidae) populations compromises the effectiveness of dengue vector
711 control in French Guiana. Mem Inst Oswaldo Cruz. 2011;106(3):346–52.

712 20. Marcombe S, Carron A, Darriet F, Etienne M, Agnew P, Tolosa M, et al. Reduced efficacy of
713 pyrethroid space sprays for dengue control in an area of Martinique with pyrethroid resistance.
714 Am J Trop Med Hyg. 2009;80(5):745–51.

715 21. Marcombe S, Darriet F, Tolosa M, Agnew P, Duchon S, Etienne M, et al. Pyrethroid resistance
716 reduces the efficacy of space sprays for dengue control on the island of Martinique (Caribbean).
717 PLoS Negl Trop Dis. 2011;5(6):e1202.

718 22. Valle D, Bellinato DF, Viana-Medeiros PF, Lima JBP, Martins Junior ADJ. Resistance to temephos
719 and deltamethrin in Aedes aegypti from Brazil between 1985 and 2017. Mem Inst Oswaldo Cruz.
720 2019;114:e180544.

721 23. Smith LB, Kasai S, Scott JG. Pyrethroid resistance in *Aedes aegypti* and *Aedes albopictus*:
722 Important mosquito vectors of human diseases. Pestic Biochem Physiol. 2016;133:1–12.

723 24. Soderlund DM. Molecular mechanisms of pyrethroid insecticide neurotoxicity: recent advances.
724 Arch Toxicol. 2012;86(2):165–81.

725 25. Auteri M, La Russa F, Blanda V, Torina A. Insecticide Resistance Associated with *kdr* Mutations in
726 *Aedes albopictus*: An Update on Worldwide Evidences. BioMed Res Int. 2018;2018:1–10.

727 26. Endersby-Harshman NM, Schmidt TL, Hoffmann AA. Diversity and distribution of sodium channel
728 mutations in *Aedes albopictus* (Diptera: Culicidae). Healy K, éditeur. J Med Entomol.
729 2024;61(3):630–43.

730 27. Soderlund DM, Knipple DC. The molecular biology of knockdown resistance to pyrethroid
731 insecticides. Insect Biochem Mol Biol. 2003;33(6):563–77.

732 28. Uemura N, Itokawa K, Komagata O, Kasai S. Recent advances in the study of knockdown
733 resistance (kdr) mutations in Aedes mosquitoes with a focus on several remarkable mutations.
734 Curr Opin Insect Sci. 2024;101178.

735 29. Chambers J. An introduction to the metabolism of pyrethroids. In: Gunther FA, Gunther JD,
736 éditeurs. Residue Reviews [Internet]. New York, NY: Springer New York; 1980. p. 101–24.
737 (Reviews of Environmental Contamination and Toxicology; vol. 73).
738 http://link.springer.com/10.1007/978-1-4612-6068-4_7

739 30. Dermauw W, Van Leeuwen T. The ABC gene family in arthropods: Comparative genomics and
740 role in insecticide transport and resistance. Insect Biochem Mol Biol. 2014;45:89–110.

741 31. Panini M, Manicardi GC, Moores GD, Mazzoni E. An overview of the main pathways of metabolic
742 resistance in insects. Invertebr Surviv J. 2016;326-335 Pages.

743 32. Faucon F, Dusfour I, Gaude T, Navratil V, Boyer F, Chandre F, et al. Identifying genomic changes
744 associated with insecticide resistance in the dengue mosquito Aedes aegypti by deep targeted
745 sequencing. Genome Res. 2015;25(9):1347–59.

746 33. Ffrench-Constant RH. The molecular genetics of insecticide resistance. Genetics.
747 2013;194(4):807–15.

748 34. Lucas ER, Miles A, Harding NJ, Clarkson CS, Lawniczak MK, Kwiatkowski DP, et al. Whole genome
749 sequencing reveals high complexity of copy number variation at insecticide resistance loci in
750 malaria mosquitoes. BioRxiv. 2018;http://dx.doi.org/10.1101/39956.

751 35. Weetman D, Djogbenou LS, Lucas E. Copy number variation (CNV) and insecticide resistance in
752 mosquitoes: evolving knowledge or an evolving problem? Curr Opin Insect Sci. 2018;27:82–8.

753 36. Chuaycharoensuk T, Juntarajumnong W, Boonyuan W, Bangs MJ, Akratanakul P, Thammapalo S,
754 et al. Frequency of pyrethroid resistance in Aedes aegypti and Aedes albopictus (Diptera:
755 Culicidae) in Thailand. J Vector Ecol. 2011;36(1):204–12.

756 37. Ishak HI, Zairi J, Ranson H, Wondji C. Contrasting patterns of insecticide resistance and
757 knockdown resistance (kdr) in the dengue vectors *Aedes aegypti* and *Aedes albopictus* from
758 Malaysia. Parasit Vectors. 2015;8:181.

759 38. Lee RML, Choong CTH, Goh BPL, Ng LC, Lam-Phua SG. Bioassay and biochemical studies of the
760 status of pirimiphos-methyl and cypermethrin resistance in Aedes (Stegomyia) aegypti and Aedes
761 (Stegomyia) albopictus (Diptera: Culicidae) in Singapore. Trop Biomed. 2014;31(4):670–9.

762 39. Thanispong K, Sathantriphop S, Malaithong N, Bangs MJ, Chareonviriyaphap T. Establishment of
763 Diagnostic Doses of Five Pyrethroids for Monitoring Physiological Resistance in Aedes Albopictus
764 in Thailand. J Am Mosq Control Assoc. 2015;31(4):346–52.

765 40. Gao JP, Chen HM, Shi H, Peng H, Ma YJ. Correlation between adult pyrethroid resistance and
766 knockdown resistance (kdr) mutations in Aedes albopictus (Diptera: Culicidae) field populations
767 in China. Infect Dis Poverty. 2018;7(1):86.

768 41. Kushwah RBS, Mallick PK, Ravikumar H, Dev V, Kapoor N, Adak TP, et al. Status of DDT and
769 pyrethroid resistance in Indian Aedes albopictus and absence of knockdown resistance (kdr)
770 mutation. J Vector Borne Dis. 2015;52(1):95–8.

771 42. Mohsin M, Naz S, Khan I, Jabeen A, Bilal H, Ahmed R, et al. Susceptibility status of Aedes aegypti
772 and Aedes albopictus against insecticides at eastern Punjab, Pakistan. Int J Mosq Res.
773 2016;3:41–6.

774 43. Kasai S, Caputo B, Tsunoda T, Cuong TC, Maekawa Y, Lam-Phua SG, et al. First detection of a Vssc
775 allele V1016G conferring a high level of insecticide resistance in Aedes albopictus collected from
776 Europe (Italy) and Asia (Vietnam), 2016: a new emerging threat to controlling arboviral diseases.
777 Euro Surveill Bull Eur Sur Mal Transm Eur Commun Dis Bull. 2019;24(5).

778 44. Zhou X, Yang C, Liu N, Li M, Tong Y, Zeng X, et al. Knockdown resistance (kdr) mutations within
779 seventeen field populations of Aedes albopictus from Beijing China: first report of a novel
780 V1016G mutation and evolutionary origins of kdr haplotypes. Parasit Vectors. 2019;12(1):180.

781 45. Ishak IH, Riveron JM, Ibrahim SS, Stott R, Longbottom J, Irving H, et al. The Cytochrome P450
782 gene CYP6P12 confers pyrethroid resistance in kdr-free Malaysian populations of the dengue
783 vector *Aedes albopictus*. Sci Rep. 2016;6:24707.

784 46. Marcombe S, Doeurk B, Thammavong P, Veseli T, Heafield C, Mills MA, et al. Metabolic
785 Resistance and Not Voltage-Gated Sodium Channel Gene Mutation Is Associated with Pyrethroid
786 Resistance of Aedes albopictus (Skuse, 1894) from Cambodia. Insects. 2024;15(5):358.

787 47. Xu J, Su X, Bonizzoni M, Zhong D, Li Y, Zhou G, et al. Comparative transcriptome analysis and RNA
788 interference reveal CYP6A8 and SNPs related to pyrethroid resistance in Aedes albopictus.
789 Attardo GM, éditeur. PLoS Negl Trop Dis. 2018;12(11):e0006828.

790 48. Pichler V, Bellini R, Veronesi R, Arnoldi D, Rizzoli A, Lia RP, et al. First evidence of resistance to
791 pyrethroid insecticides in Italian *AEDES ALBOPICTUS* populations 26 years after invasion. Pest
792 Manag Sci. 2018;74(6):1319–27.

793 49. Pichler V, Malandruccolo C, Paola S, Bellini R, Severini F, Toma L, et al. Phenotypic and genotypic
794 pyrethroid resistance of Aedes albopictus, with focus on the 2017 chikungunya outbreak in Italy.
795 Pest Manag Sci. 2019;

796 50. Pichler V, Caputo B, Valadas V, Micocci M, Horvath C, Virgillito C, et al. Geographic distribution of
797 the V1016G knockdown resistance mutation in Aedes albopictus: a warning bell for Europe.
798 Parasit Vectors. 2022;15(1):280.

799 51. Djiappi-Tchamen B, Nana-Ndjangwo MS, Mavridis K, Talipouo A, Nchoutpouen E, Makoudjou I, et
800 al. Analyses of Insecticide Resistance Genes in Aedes aegypti and Aedes albopictus Mosquito
801 Populations from Cameroon. Genes. 2021;12(6):828.

802 52. Yamashita S, Uruma K, Yang C, Higa Y, Minakawa N, Cuamba N, et al. The origin and insecticide
803 resistance of Aedes albopictus mosquitoes established in southern Mozambique. Parasit Vectors.
804 2024;17(1):292.

805 53. Yougang AP, Keumeni CR, Wilson-Bahun TA, Tedjou AN, Njiokou F, Wondji C, et al. Spatial
806 distribution and insecticide resistance profile of Aedes aegypti and Aedes albopictus in Douala,
807 the most important city of Cameroon. Moreira LA, éditeur. PLOS ONE. 2022;17(12):e0278779.

808 54. Delatte H, Dehecq JS, Thiria J, Domerg C, Paupy C, Fontenille D. Geographic Distribution and
809 Developmental Sites of *Aedes albopictus* (Diptera: Culicidae) During a Chikungunya Epidemic
810 Event. Vector-Borne Zoonotic Dis. 2008;8(1):25–34.

811 55. Delatte H, Paupy C, Dehecq JS, Thiria J, Failloux AB, Fontenille D. *Aedes albopictus* , vecteur des
812 virus du chikungunya et de la dengue à la Réunion : biologie et contrôle. Parasite.
813 2008;15(1):3–13.

814 56. Renault P, Solet JL, Sissoko D, Balleydier E, Larrieu S, Filleul L, et al. A major epidemic of
815 chikungunya virus infection on Reunion Island, France, 2005-2006. Am J Trop Med Hyg.
816 2007;77(4):727–31.

817 57. Vincent M, Paty MC, Gerardin P, Balleydier E, Etienne A, Daoudi J, et al. From dengue outbreaks
818 to endemicity: Reunion Island, France, 2018 to 2021. Eurosurveillance. 2023;28(29).

819 58. Saisine ANSES n°2020-SA-0029. Résistance des moustiques vecteurs aux insecticides. 2020.
820 https://www.anses.fr/fr/system/files/BIOCIDES2020SA0029Ra.pdf

821 59. Tancredi A, Papandrea D, Marconcini M, Carballar-Lejarazu R, Casas-Martinez M, Lo E, et al.
822 Tracing temporal and geographic distribution of resistance to pyrethroids in the arboviral vector
823 Aedes albopictus. Aldridge RL, éditeur. PLoS Negl Trop Dis. 2020;14(6):e0008350.

824 60. Chandor-Proust A, Bibby J, Regent-Kloeckner M, Roux J, Guittard-Crilat E, Poupardin R, et al. The
825 central role of mosquito cytochrome P450 CYP6Zs in insecticide detoxification revealed by
826 functional expression and structural modelling. Biochem J. 2013;455:75–85.

827 61. Nikou D, Ranson H, Hemingway J. An adult-specific CYP6P450 gene is overexpressed in a
828 pyrethroid-resistant strain of the malaria vector, Anopheles gambiae. Gene. 2003;318:91–102.

829 62. Vontas J, Katsavou E, Mavridis K. Cytochrome P450-based metabolic insecticide resistance in
830 Anopheles and Aedes mosquito vectors: Muddying the waters. Pestic Biochem Physiol.
831 2020;170:104666.

832 63. Stevenson BJ, Bibby J, Pignatelli P, Muangnoicharoen S, O'Neill PM, Lian LY, et al. Cytochrome
833 P450 6M2 from the malaria vector *Anopheles gambiae* metabolizes pyrethroids: Sequential
834 metabolism of deltamethrin revealed. Insect Biochem Mol Biol. 2011;41(7):492–502.

835 64. Kouamo MFM, Ibrahim SS, Hearn J, Riveron JM, Kusimo M, Tchouakui M, et al. Genome-Wide
836 Transcriptional Analysis and Functional Validation Linked a Cluster of Epsilon Glutathione S-
837 Transferases with Insecticide Resistance in the Major Malaria Vector Anopheles funestus across
838 Africa. Genes. 2021;12(4):561.

839 65. Messenger LA, Impoinvil LM, Derilus D, Yewhalaw D, Irish S, Lenhart A. A whole transcriptomic
840 approach provides novel insights into the molecular basis of organophosphate and pyrethroid
841 resistance in Anopheles arabiensis from Ethiopia. Insect Biochem Mol Biol. 2021;139:103655.

842 66. Simma EA, Dermauw W, Balabanidou V, Snoeck S, Bryon A, Clark RM, et al. Genome-wide gene
843 expression profiling reveals that cuticle alterations and P450 detoxification are associated with
844 deltamethrin and DDT resistance in Anopheles arabiensis populations from Ethiopia. Pest Manag
845 Sci. 2019;75(7):1808–18.

846 67. Tao F, Si F, Hong R, He X, Li X, Qiao L, et al. Glutathione *S* -transferase (GST) genes and their
847 function associated with pyrethroid resistance in the malaria vector *Anopheles sinensis*. Pest
848 Manag Sci. 2022;78(10):4127–39.

849 68. Bariami V, Jones CM, Poupardin R, Vontas J, Ranson H. Gene Amplification, ABC Transporters and
850 Cytochrome P450s: Unraveling the Molecular Basis of Pyrethroid Resistance in the Dengue
851 Vector, Aedes aegypti. PLoS Negl Trop Dis. 2012;6(6).

852 69. Bonizzoni M, Afrane Y, Dunn WA, Atieli FK, Zhou G, Zhong D, et al. Comparative transcriptome
853 analyses of deltamethrin-resistant and -susceptible Anopheles gambiae mosquitoes from Kenya
854 by RNA-Seq. PloS One. 2012;7(9):e44607.

855 70. Epis S, Porretta D, Mastrantonio V, Urbanelli S, Sassera D, De Marco L, et al. Temporal dynamics
856 of the ABC transporter response to insecticide treatment: insights from the malaria vector
857 Anopheles stephensi. Sci Rep. 2014;4(1):7435.

858 71. He Q, Yan Z, Si F, Zhou Y, Fu W, Chen B. ATP-Binding Cassette (ABC) Transporter Genes Involved
859 in Pyrethroid Resistance in the Malaria Vector Anopheles sinensis: Genome-Wide Identification,
860 Characteristics, Phylogenetics, and Expression Profile. Int J Mol Sci. 2019;20(6):1409.

861 72. Mastrantonio V, Ferrari M, Epis S, Negri A, Scuccimarra G, Montagna M, et al. Gene expression
862 modulation of ABC transporter genes in response to permethrin in adults of the mosquito
863 malaria vector Anopheles stephensi. Acta Trop. 2017;171:37–43.

864 73. Xu J, Zheng J, Zhang R, Wang H, Du J, Li J, et al. Identification and functional analysis of ABC
865 transporter genes related to deltamethrin resistance in *Culex pipiens pallens*. Pest Manag Sci.
866 2023;79(10):3642–55.

867 74. Scheuer T. Regulation of sodium channel activity by phosphorylation. Semin Cell Dev Biol.
868 2011;22(2):160–5.

869 75. Srinivasan Y, Elmer L, Davis J, Bennett V, Angelides K. Ankyrin and spectrin associate with voltage-
870 dependent sodium channels in brain. Nature. 1988;333(6169):177–80.

871 76. Manni M, Guglielmino CR, Scolari F, Vega-Rua A, Failloux AB, Somboon P, et al. Genetic evidence
872 for a worldwide chaotic dispersion pattern of the arbovirus vector, Aedes albopictus. PLoS Negl
873 Trop Dis. 2017;11(1):e0005332.

874 77. Maynard AJ, Ambrose L, Cooper RD, Chow WK, Davis JB, Muzari MO, et al. Tiger on the prowl:
875 Invasion history and spatio-temporal genetic structure of the Asian tiger mosquito Aedes
876 albopictus (Skuse 1894) in the Indo-Pacific. Vasilakis N, éditeur. PLoS Negl Trop Dis.
877 2017;11(4):e0005546.

878 78. Mousson L, Dauga C, Garrigues T, Schaffner F, Vazeille M, Failloux AB. Phylogeography of *Aedes* (
879 *Stegomyia*) *aegypti* (L.) and *Aedes* (*Stegomyia*) *albopictus* (Skuse) (Diptera: Culicidae) based on
880 mitochondrial DNA variations. Genet Res. 2005;86(1):1–11.

881 79. Chen H, Li K, Wang X, Yang X, Lin Y, Cai F, et al. First identification of kdr allele F1534S in VGSC
882 gene and its association with resistance to pyrethroid insecticides in Aedes albopictus
883 populations from Haikou City, Hainan Island, China. Infect Poverty. 2016;5:31.

884 80. David JP, Ismail HM, Chandor-Proust A, Paine MJ. Role of cytochrome P450s in insecticide
885 resistance: impact on the control of mosquito-borne diseases and use of insecticides on Earth.
886 Philos Trans R Soc Lond B Biol Sci. 2013;368(1612):20120429.

887 81. Bengoa M, Eritja R, Delacour S, Miranda MA, Sureda A, Lucientes J. First Data on Resistance to
888 Pyrethroids in Wild Populations of Aedes albopictus from Spain. J Am Mosq Control Assoc.
889 2017;33(3):246–9.

890 82. Chen HM. Role of metabolic detoxification enzyme activity and knockdown resistance gene
891 mutations in resistance of aedes albopictus to pyrethroid insecticides. Acad J Second Mil Med
892 Univ. 2019;512–9.

893 83. Khan HAA. Resistance to insecticides and synergism by enzyme inhibitors in Aedes albopictus
894 from Punjab, Pakistan. Sci Rep. 2020;10(1):21034.

895 84. Li Y, Xu J, Zhong D, Zhang H, Yang W, Zhou G, et al. Evidence for multiple-insecticide resistance in
896 urban Aedes albopictus populations in southern China. Parasit Vectors. 2018;11(1):4.

897 85. Feyereisen R. Insect P450 enzymes. Annu Rev Entomol. 1999;44:507–33.

898 86. Bacot T, Haberkorn C, Guilliet J, Cattel J, Kefi M, Nadalin L, et al. A genomic duplication spanning
899 multiple P450s contributes to insecticide resistance in the dengue mosquito Aedes aegypti. Peer
900 Community J. 2024;4:e110.

901 87. Cattel J, Haberkorn C, Laporte F, Gaude T, Cumer T, Renaud J, et al. A genomic amplification
902 affecting a carboxylesterase gene cluster confers organophosphate resistance in the mosquito
903 *Aedes aegypti*: From genomic characterization to high-throughput field detection. Evol Appl.
904 2021;14(4):1009–22.

905 88. Remnant EJ, Good RT, Schmidt JM, Lumb C, Robin C, Daborn PJ, et al. Gene duplication in the
906 major insecticide target site, *Rdl* , in *Drosophila melanogaster*. Proc Natl Acad Sci.
907 2013;110(36):14705–10.

908 89. Melo ESD, Wallau GL. Mosquito genomes are frequently invaded by transposable elements
909 through horizontal transfer. Malik HS, éditeur. PLOS Genet. 2020;16(11):e1008946.

910 90. Nene V, Wortman JR, Lawson D, Haas B, Kodira C, Tu ZJ, et al. Genome sequence of *Aedes*
911 *aegypti*, a major arbovirus vector. Science. 2007;316(5832):1718–23.

912 91. Palatini U, Masri RA, Cosme LV, Koren S, Thibaud-Nissen F, Biedler JK, et al. Improved reference
913 genome of the arboviral vector Aedes albopictus. Genome Biol. 2020;21(1):215.

914 92. Amezian D, Nauen R, Le Goff G. Transcriptional regulation of xenobiotic detoxification genes in
915 insects - An overview. Pestic Biochem Physiol. 2021;174:104822.

916 93. Ji M, Vandenhole M, De Beer B, De Rouck S, Villacis-Perez E, Feyereisen R, et al. A nuclear
917 receptor HR96-related gene underlies large trans-driven differences in detoxification gene
918 expression in a generalist herbivore. Nat Commun. 2023;14(1):4990.

919 94. Wen X, Feng K, Qin J, Wei P, Cao P, Zhang Y, et al. A detoxification pathway initiated by a nuclear
920 receptor TcHR96h in Tetranychus cinnabarinus (Boisduval). Palli SR, éditeur. PLOS Genet.
921 2023;19(9):e1010911.

922 95. Lien NTK, Ngoc NTH, Lan NN, Hien NT, Tung NV, Ngan NTT, et al. Transcriptome Sequencing and
923 Analysis of Changes Associated with Insecticide Resistance in the Dengue Mosquito (Aedes
924 aegypti) in Vietnam. Am J Trop Med Hyg. 2019;100(5):1240–8.

925 96. Shan G, Hammock BD. Development of Sensitive Esterase Assays Based on α-Cyano-Containing
926 Esters. Anal Biochem. 2001;299(1):54–62.

927 97. Faria R, Johannesson K, Butlin RK, Westram AM. Evolving Inversions. Trends Ecol Evol.
928 2019;34(3):239–48.

929 98. Haberkorn C, David J, Henri H, Delpuech J, Lasseur R, Vavre F, et al. A major 6 Mb superlocus is
930 involved in pyrethroid resistance in the common bed bug *Cimex lectularius*. Evol Appl.
931 2023;16(5):1012–28.

932 99. Wellenreuther M, Mérot C, Berdan E, Bernatchez L. Going beyond SNPs: The role of structural
933 genomic variants in adaptive evolution and species diversification. Mol Ecol. 2019;28(6):1203–9.

934 100. Wellenreuther M, Bernatchez L. Eco-Evolutionary Genomics of Chromosomal Inversions. Trends
935 Ecol Evol. 2018;33(6):427–40.

936 101. Deng J, Guo Y, Su X, Liu S, Yang W, Wu Y, et al. Impact of deltamethrin-resistance in Aedes
937 albopictus on its fitness cost and vector competence. Churcher TS, éditeur. PLoS Negl Trop Dis.
938 2021;15(4):e0009391.

939 102. Standard operating procedure for testing insecticide susceptibility of adult mosquitoes in WHO
940 tube tests. SOP version: WHO Tube test/01/14. World Health Organization; 2022.
941 https://iris.who.int/bitstream/handle/10665/352316/9789240043831-eng.pdf?sequence=1

942 103. Boyle JH, Rastas PMA, Huang X, Garner AG, Vythilingam I, Armbruster PA. A Linkage-Based
943 Genome Assembly for the Mosquito Aedes albopictus and Identification of Chromosomal
944 Regions Affecting Diapause. Insects. 2021;12(2):167.

945 104. Chen Y, Chen Y, Shi C, Huang Z, Zhang Y, Li S, et al. SOAPnuke: a MapReduce acceleration-
946 supported software for integrated quality control and preprocessing of high-throughput
947 sequencing data. GigaScience. 2018;7(1):1-6.

948 105. Andrews S. FastQC: a quality control tool for high throughput sequence data. 2010. Available
949 online at: http://www.bioinformatics.babraham.ac.uk/projects/fastqc/

950 106. Dobin A, Davis CA, Schlesinger F, Drenkow J, Zaleski C, Jha S, et al. STAR: ultrafast universal RNA-
951 seq aligner. Bioinformatics. 2013;29(1):15–21.

952 107. Benjamini Y, Hochberg Y. Controlling the False Discovery Rate: a Practical and Powerful Approach
953 to Multiple Testing. J R Stat Soc B. 1995;57:289–300.

954 108. Giraldo-Calderón GI, Harb OS, Kelly SA, Rund SS, Roos DS, McDowell MA. VectorBase.org
955 updates: bioinformatic resources for invertebrate vectors of human pathogens and related
956 organisms. Curr Opin Insect Sci. 2022;50:100860.

957 109. Harb OS, McDowell MA, Roos DS. VEuPathDB Resources: A Platform for Free Online Data
958 Exploration, Integration, and Analysis. In: Setubal JC, Stadler PF, Stoye J, éditeurs. Comparative
959 Genomics. New York, NY: Springer US; 2024 p. 573–86. (Methods in Molecular Biology; vol.
960 2802).

961 110. Lemoine F, Correia D, Lefort V, Doppelt-Azeroual O, Mareuil F, Cohen-Boulakia S, et al.
962 NGPhylogeny.fr: new generation phylogenetic services for non-specialists. Nucleic Acids Res.
963 2019;47(W1):W260–5.

964 111. Sacomoto GA, Kielbassa J, Chikhi R, Uricaru R, Antoniou P, Sagot MF, et al. KIS SPLICE: de-novo
965 calling alternative splicing events from RNA-seq data. BMC Bioinformatics. 2012;13(S6):S5.

966 112. Benoit-Pilven C, Marchet C, Chautard E, Lima L, Lambert MP, Sacomoto G, et al. Complementarity
967 of assembly-first and mapping-first approaches for alternative splicing annotation and
968 differential analysis from RNAseq data. Sci Rep. 2018;8(1):4307.

969 113. Li H, Durbin R. Fast and accurate short read alignment with Burrows-Wheeler transform.
970 Bioinformatics. 2009;25(14):1754–60.

971 114. Li H, Handsaker B, Wysoker A, Fennell T, Ruan J, Homer N, et al. The Sequence Alignment/Map
972 format and SAMtools. Bioinforma Oxf Engl. 2009;25(16):2078–9.

973 115. Schrider DR, BEGUN DJ, HAHN MW. Detecting highly differentiated copy-number variants from
974 pooled population sequencing. Pac Symp Biocomput Pac Symp Biocomput. 2013;344–55.

975 116. Danecek P, Bonfield JK, Liddle J, Marshall J, Ohan V, Pollard MO, et al. Twelve years of SAMtools
976 and BCFtools. Gigascience. 2021;10(2):giab008.

977 117. Cingolani P, Platts A, Wang LL, Coon M, Nguyen T, Wang L, et al. A program for annotating and
978 predicting the effects of single nucleotide polymorphisms, SnpEff: SNPs in the genome of
979 Drosophila melanogaster strain w^{1118}; iso-2; iso-3. Fly (Austin). 2012;6(2):80–92.

980 118. Lin L qun, Chen Y hui, Tian Y fan, Chen Y sen, Zheng Z yang, Wu J xin, et al. Study on the cross-
981 resistance of Aedes albopictus (Skuse) (Diptera: Culicidae) to deltamethrin and pyriproxyfen.
982 Parasit Vectors. 2024;17(1):403.